Combined strong and weak gravitational lensing mass measurements in galaxy clusters

Davide Abriola, PhD student, Unimi

Supervisor: Prof. Marco Lombardi
Co-supervisor: Prof. Claudio Grillo

UNIVERSITÀ
DEGLI STUDI
DI MILANO

LA STATALE

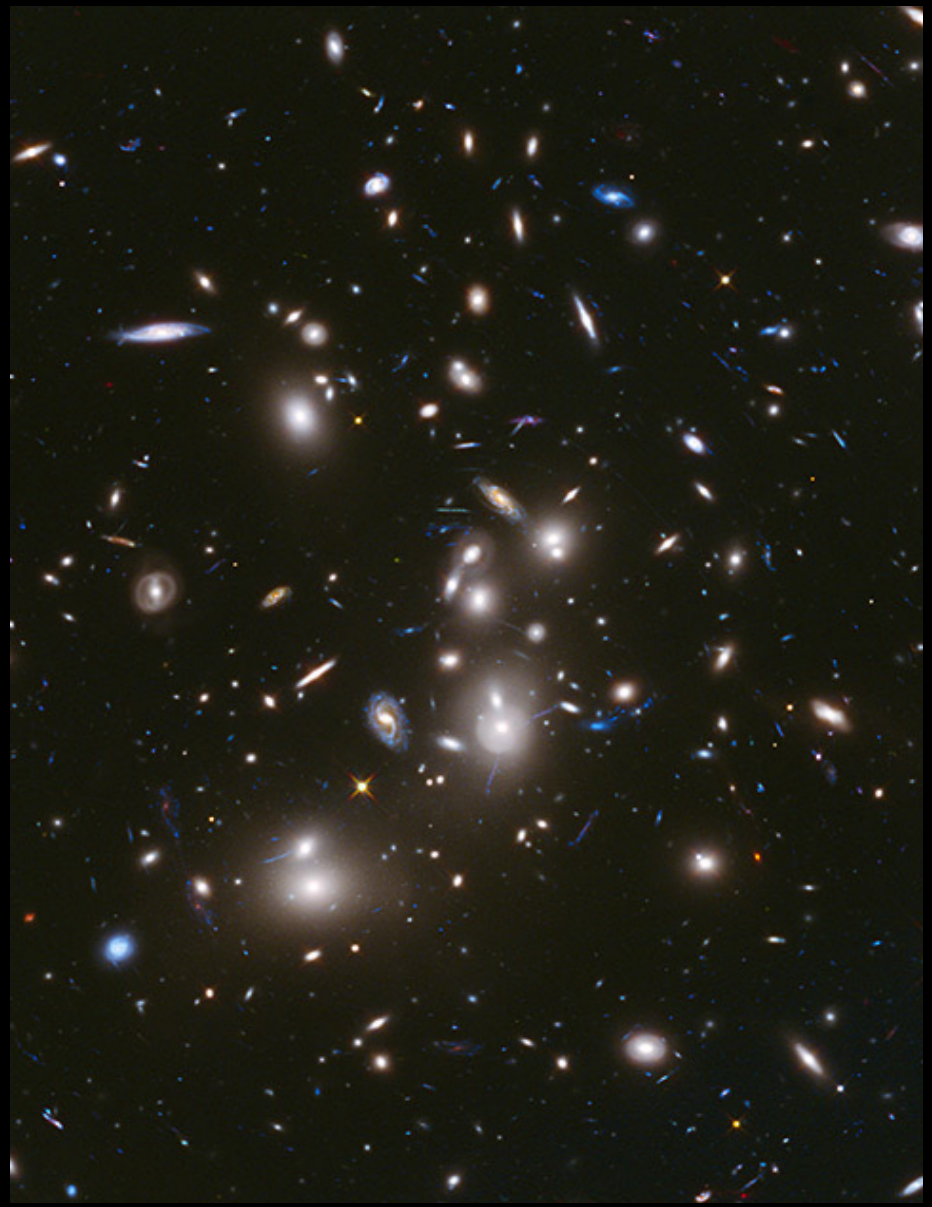

Abell 2744 as seen by the Advanced Camera for Surveys (ACS) @Hubble

Gravitational lensing in **galaxy clusters** is one of the most accurate methods to probe the **dark matter** mass distribution inside such systems and test the ΛCDM cosmological paradigm.

Whereas **strong lensing** (SL) provides a parametric mass reconstruction in the inner regions of clusters, **weak lensing** (WL) yields a complementary non-parametric reconstruction in the outskirts.

A **combined SL&WL analysis** thus provides us with unique insight and a consistent picture of the total mass distribution of these large gravitationally-bound systems. In my talk, I will present the combined analysis for the **galaxy cluster Abell 2744**.

In particular, in order to reconstruct the total mass distribution of the lens through WL, we have to :

- Detect the **sources** on the field of view;
  - Star/Galaxy separation
  - Background and cluster galaxies identification
- Reconstruct the **spatial variation** of the **PSF**; → *MCCD* (Liaudat et al., 2021)
- Measure the **ellipticities** of the background galaxies; → *NGMix* (Sheldon, 2015)
- Determine the **mass distribution** of the lens given the shear field;

We performed a WL analysis of the galaxy cluster **Abell 2744** (R. A. = $00^h : 14^m : 18.9^s$, DEC. = −30° : 23’ : 22’’) lying at redshift $z \approx 0.308$, working with data collected by **Magellan** in three bands: *g*, *r* and *i*.

Filter	Exp. time [10^4 s]	Seeing [’’]	m_{zp}
g	2.04	0.345	33.78
r	1.20	0.316	33.70
i	4.80	0.330	32.93

Pixel scale: 0.15”

Effective field of view covered: ≈ 31’ x 33’

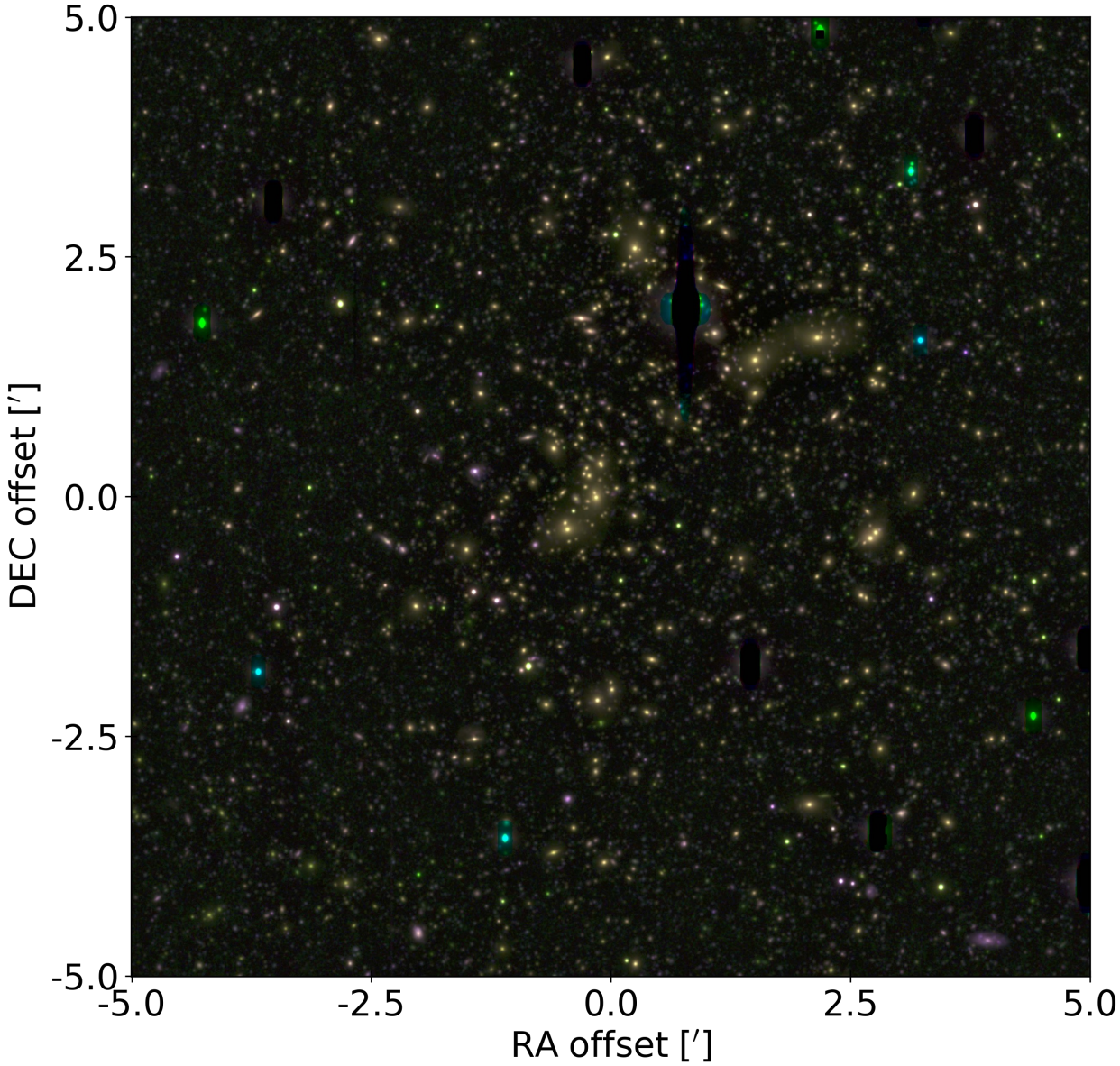

A 10’ x 10’ extract of the colour composite image of the field of view analysed (with Subaru). The cluster Abell 2744 lies at the centre of the image. Curtesy of Daniele Della Pergola.

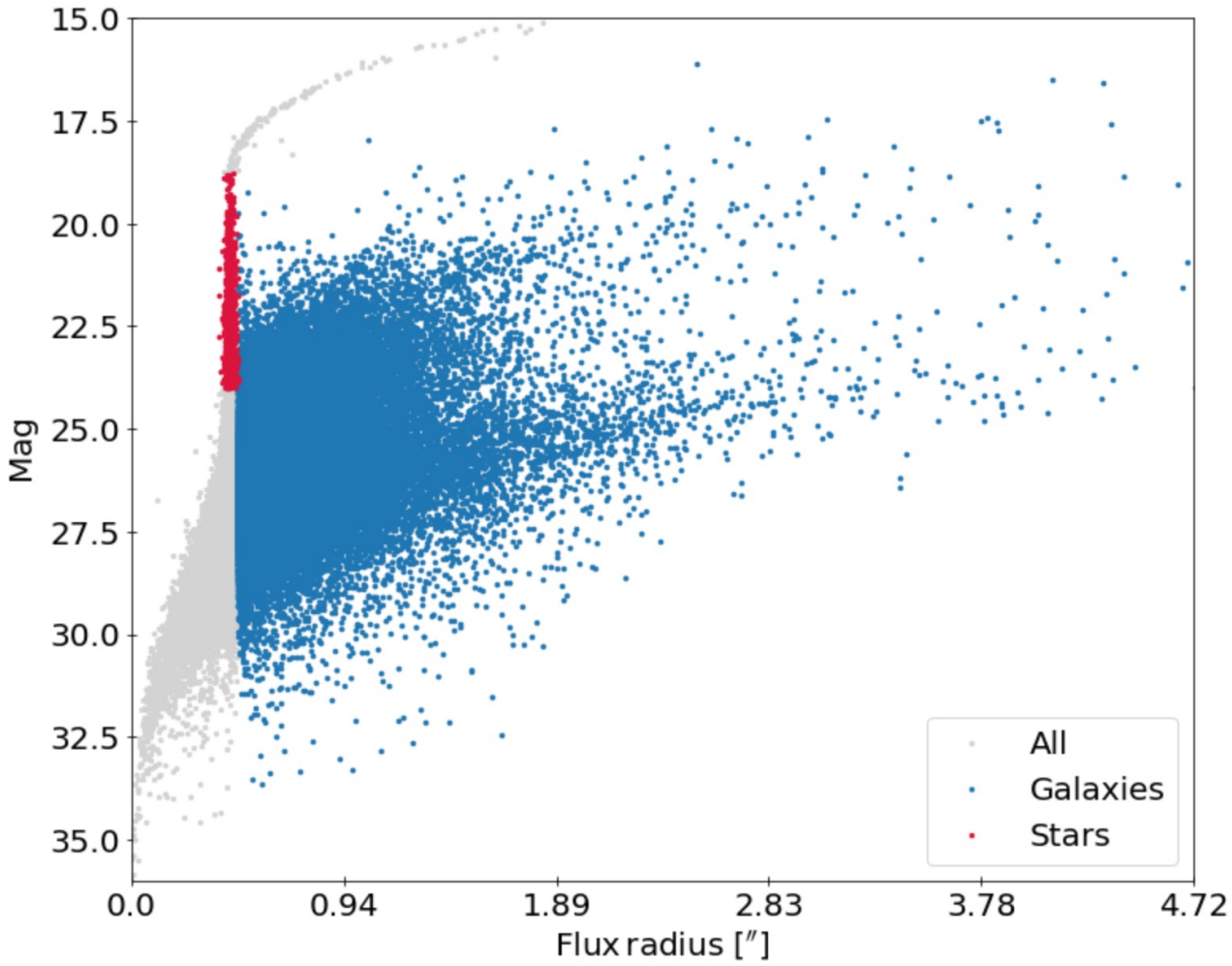

A magnitude vs. size diagram used to classify the detected sources.

We first detected sources with **Sextractor** (Bertin and Arnouts, 1996): we identified 117.001 sources that we classified into 4 categories given their distribution in size and magnitude.

After comparing the catalogs in the three bands, we identified 695 stars and 86.945 galaxies.

We distinguished cluster members and background galaxies by studying their distribution in a **color-color diagram** (see Medezinski et al., 2010; 2016).

We verified the precision and accuracy of our classification by comparing our sample to the redshift catalogue of Bergamini et al., 2022. We obtained an accuracy of ≈ 93% and a precision of ≈ 83%.

	C_z	NC_z
C	151	29
NC	50	967

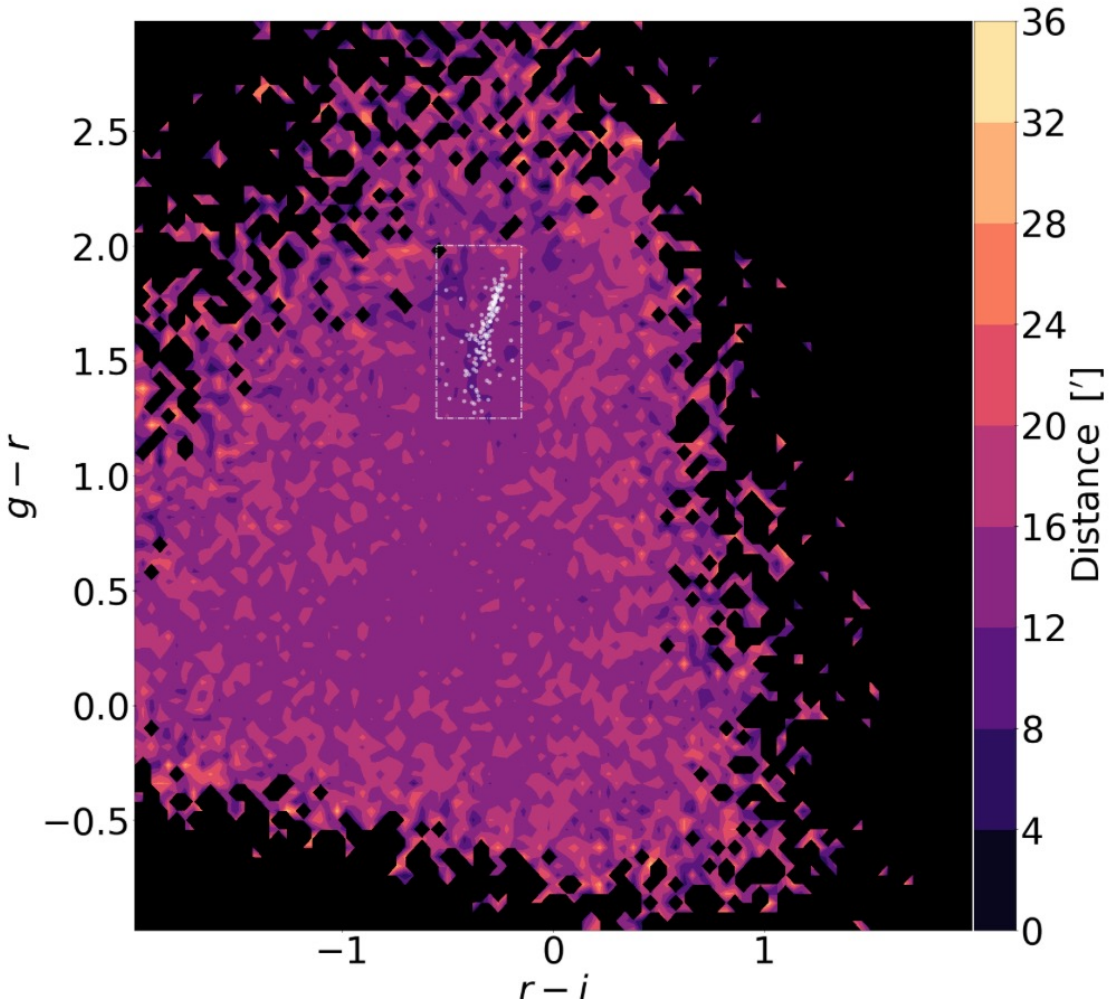

The mean distance of the galaxies from the centre of the image in a color-color space. White dots represent the spectroscopically confirmed cluster members.

The 1477 galaxies likely belonging to the cluster define a clearly visible **red cluster sequence**.

We reconstructed the **surface brightness distribution** of the cluster in the rest-frame (K-corrected) bands (see Beare et al., 2014).

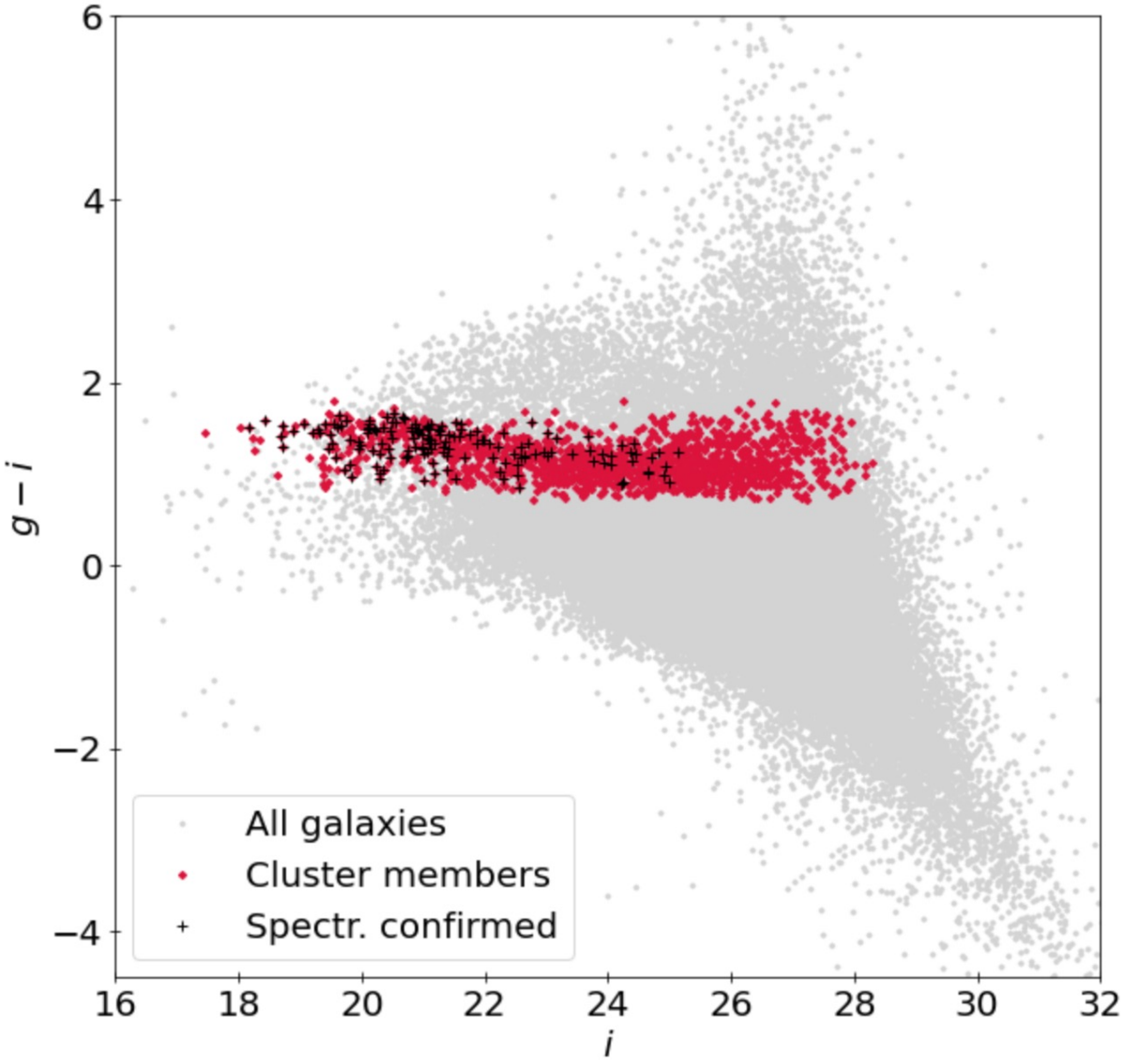

To determine background and foreground galaxies, we relied once again on the method by Medezinski et al., 2010.

Background galaxies occupy the lowest region in the color-color space; **foreground galaxies** lie in the central overdensity. We identifed more than 54.000 background galaxies.

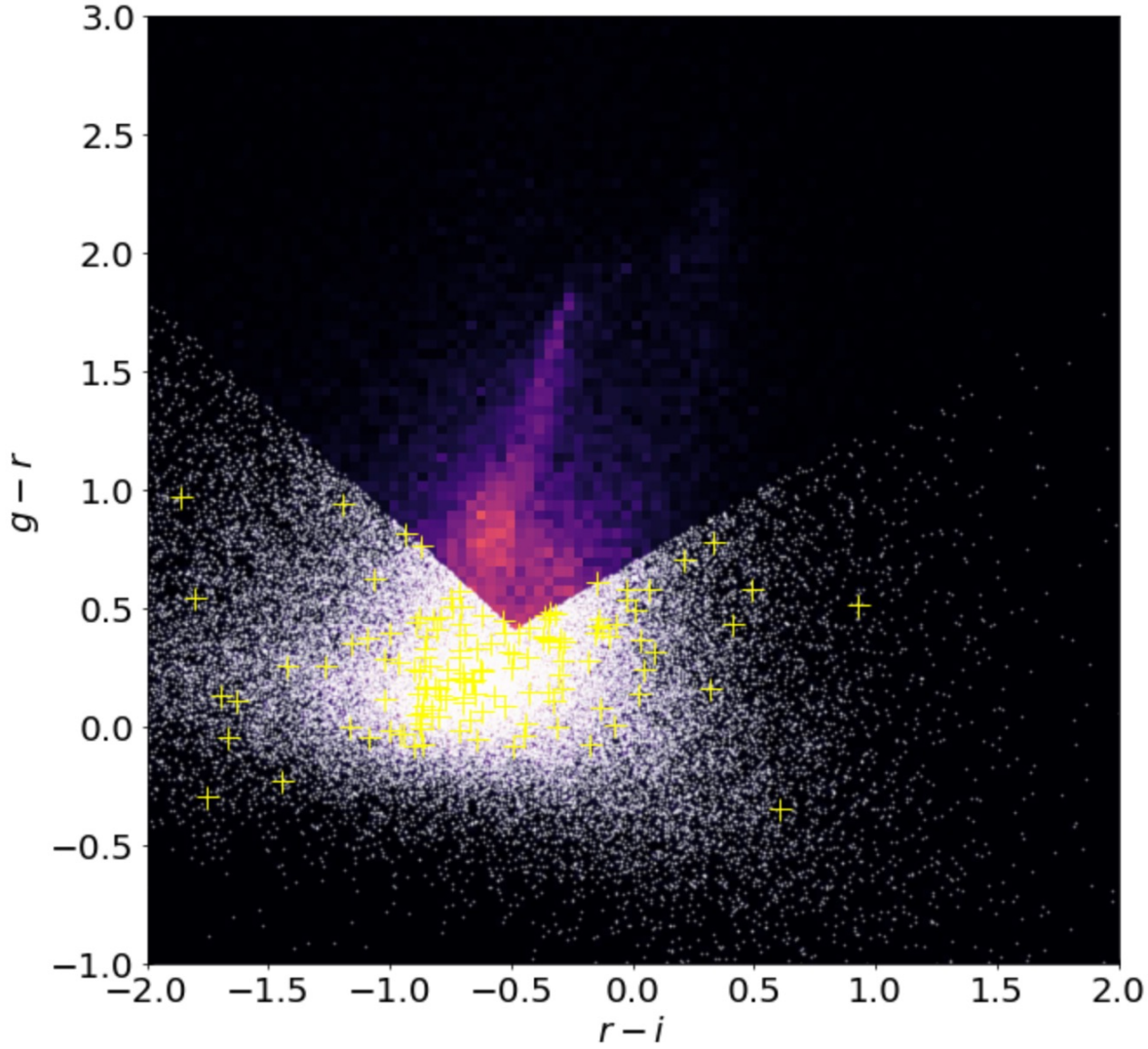

The distribution of the identified galaxies in a color-color space. Yellow crosses denote the spectroscopically confirmed background galaxies.

We reconstructed the spatial variation of the PSF with MCCD, using the identified stars.

We then applied NGMix in the **multi-band** configuration to measure the ellipticities of the background galaxies.

The results depicted here refer to the tests carried out on the **Subaru** multi-band data.

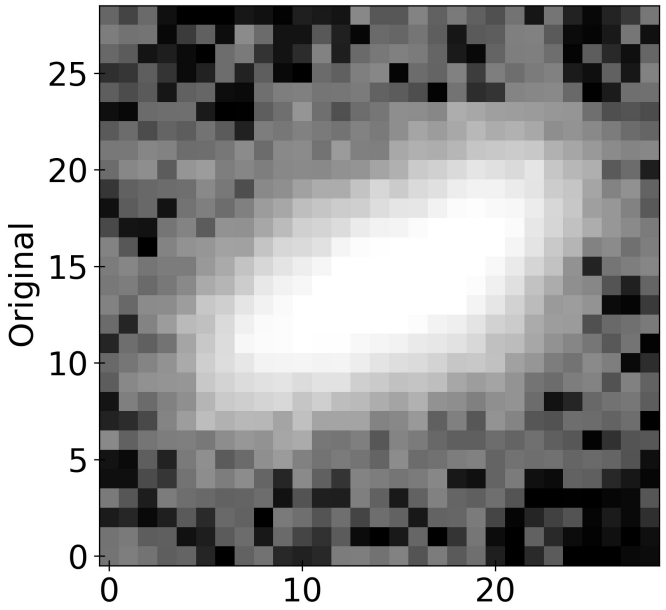

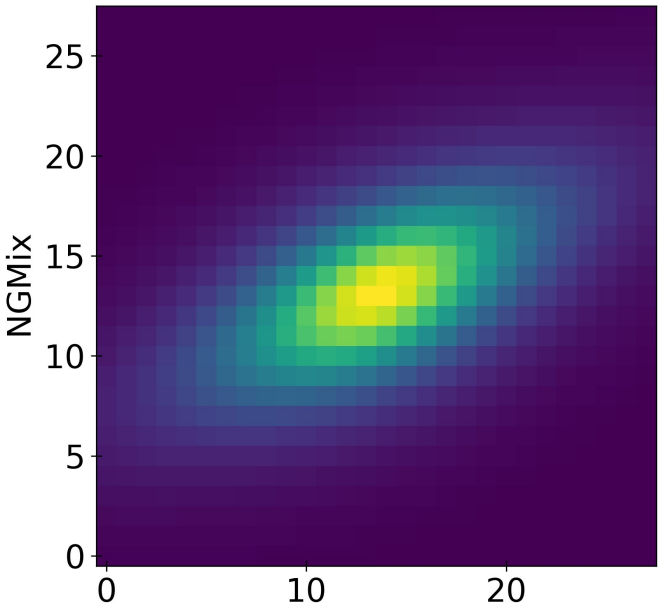

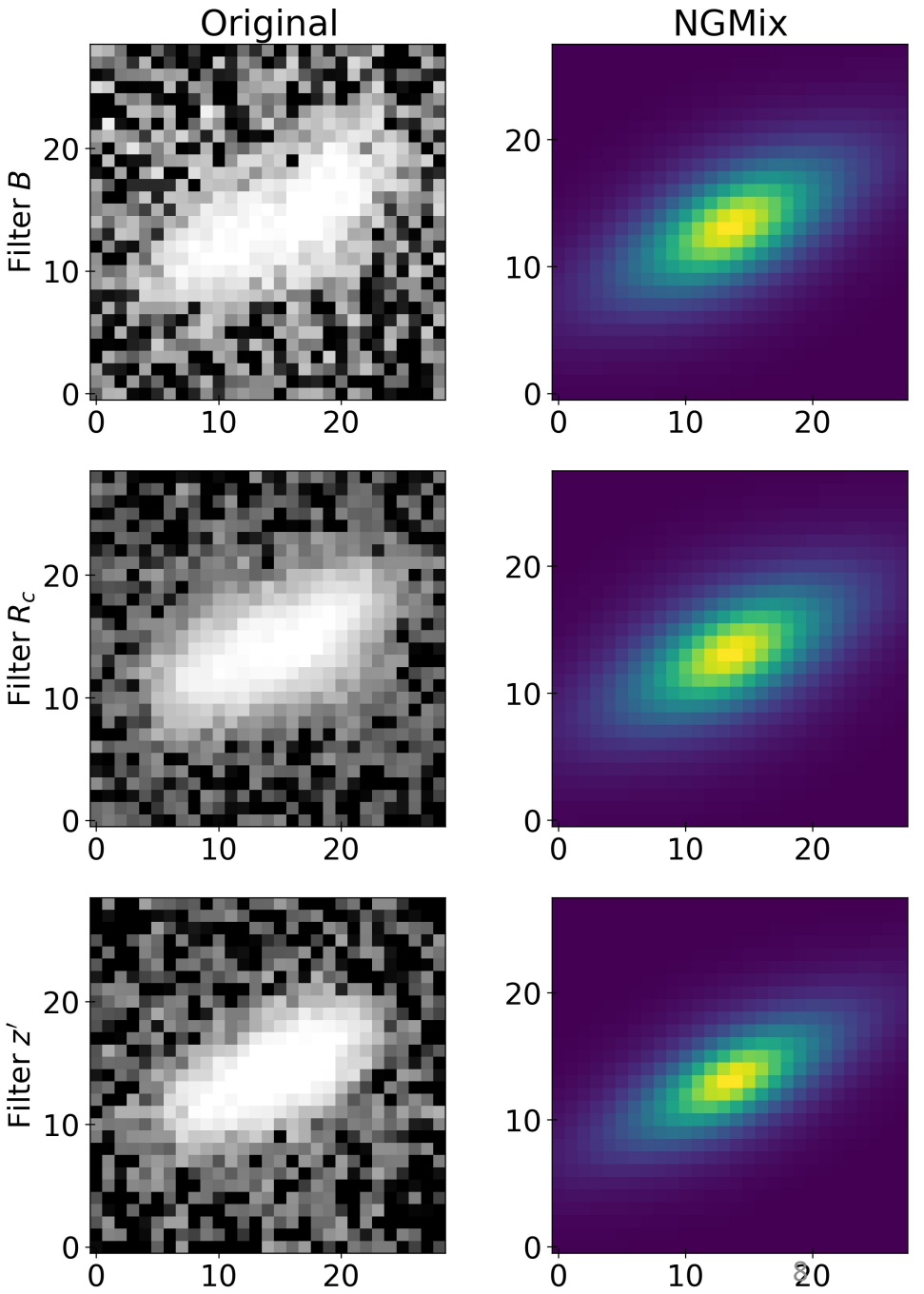

We reconstructed the **shear field** $\gamma(\vec{x})$ over a 480 x 500 px. grid, with a size of 0.1'. We estimated a "dimensional" shear $\boldsymbol{\upsilon}$ (in $M_\odot/Mpc^2$) as:

$$\upsilon(\vec{x}) = \frac{\sum_n K(\vec{x}, \vec{x}_n) \frac{1}{\sigma_n^2} S_n \varepsilon_n}{\sum_n K(\vec{x}, \vec{x}_n) \frac{1}{\sigma_n^2} S_n^2 \varepsilon_n}$$

K Gaussian kernel depending on the distance between the position on the grid $\vec{x}$ and the position of the *n*th background galaxy $\vec{x}_n$

ε_n ellipticity of the *n*th background galaxy

σ_n uncertainty on the ellipticity of the *n*th background galaxy

S_n average value of the inverse of the critical sigma for the *n*th background galaxy

To estimate the critical sigma, we took into account the **redshift distribution** of the sources. We used as a reference a photometric redshift catalogue around the HDF-N (Yang et al., 2014).

$$S_i = \left\langle \frac{1}{\Sigma_{cr}} \right\rangle_i = \frac{1}{N_i} \sum_{j=1}^{N_i} \frac{1}{\Sigma_{cr}}(z_j)$$

z_j redshift of the jth catalogue galaxy with magnitude m in $[m_i, m_i + 0.5)$ in a given band.

N_i number of catalogue galaxies with magnitude in $[m_i, m_i + 0.5)$ in a given band.

We assigned each bkg galaxy with magnitude in $[m_i, m_i + 0.5)$ the corresponding S_i

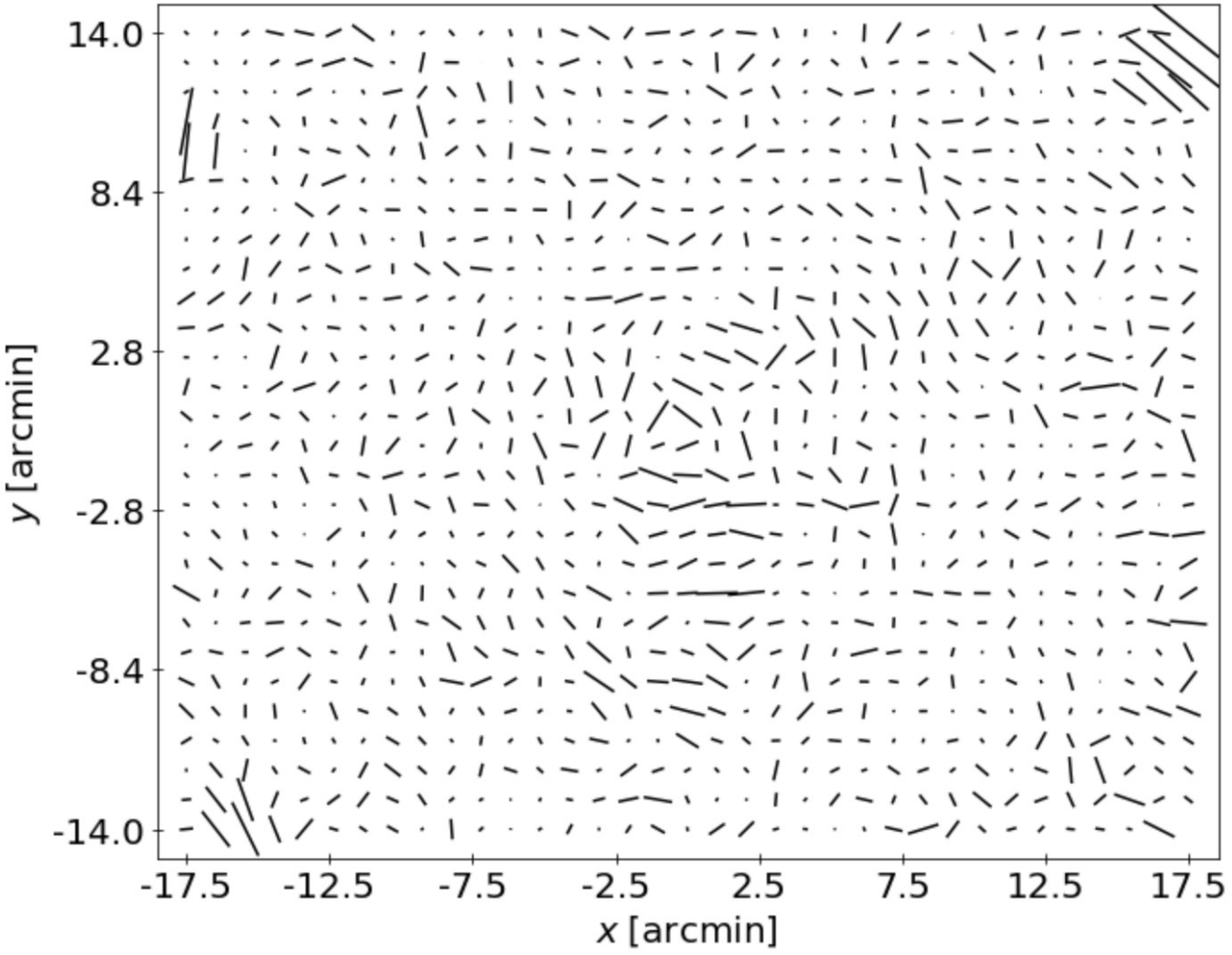

The shear field, here depicted on a smaller grid for visibility.

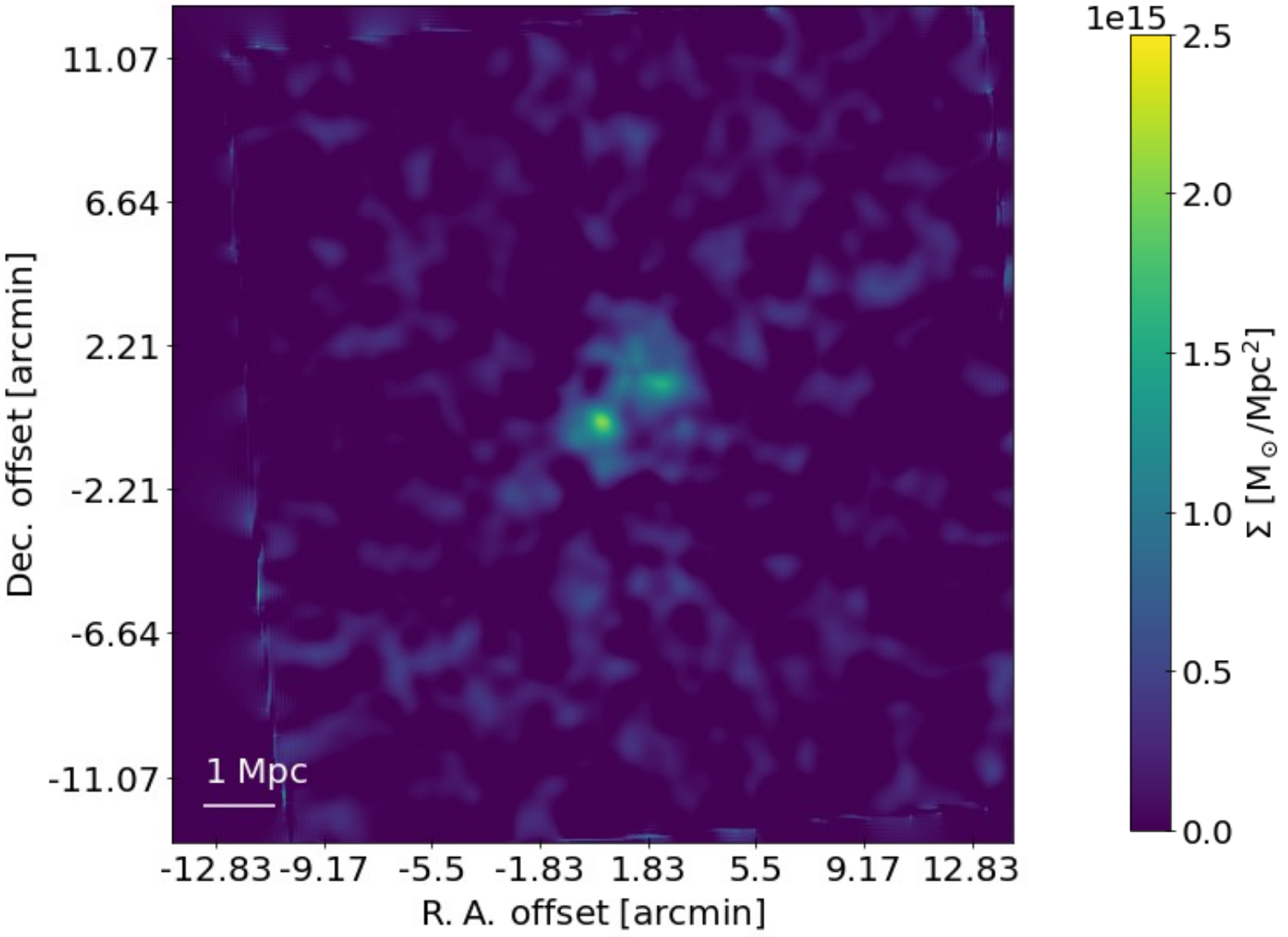

We thus reconstructed the surface mass distribution **Σ** by minimising the action (see Lombardi & Bertin, 1999):

$$S = \int \|\nabla\Sigma(\vec{x}) - \vec{u}(\vec{x})\|^2 d^2x$$

$$\vec{u} = \begin{pmatrix} v_{1,1} + v_{2,2} \\ v_{2,1} - v_{1,2} \end{pmatrix}$$

$$G\Sigma = u$$

Sparse matrix

We estimated the uncertainty on the convergence map through a ***reshuffling*** procedure, i.e., we produced further 120 **Σ** maps each time shuffling the coordinates of the background galaxies.

We studied possible systematic effects by evaluating the **B-modes**. The signal is consistent with zero ($\sigma_B \approx 0.1 \times 10^{14}\ M_\odot$).

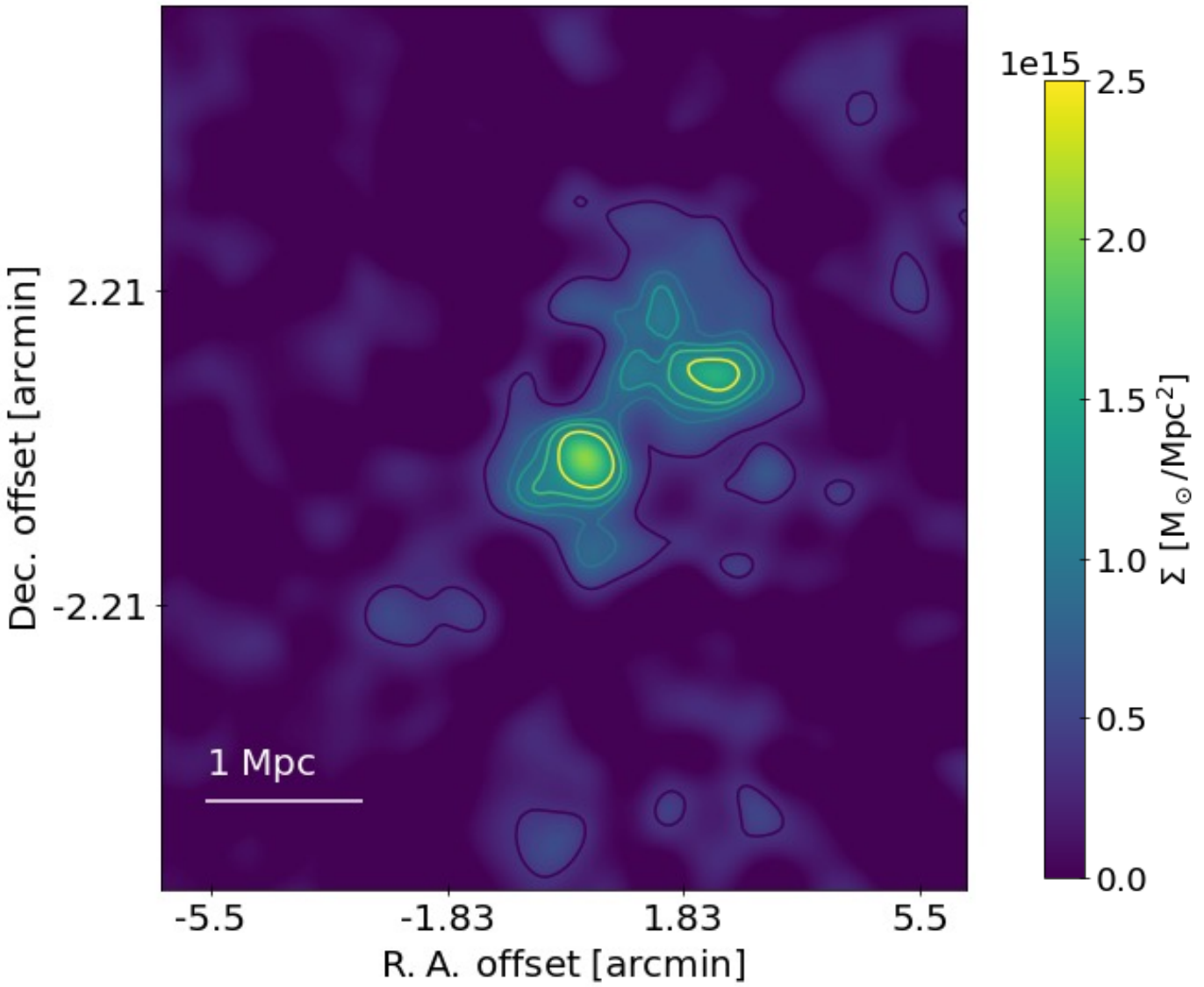

An extract of the convergence map with overlaid the contour lines corresponding to 2.5, 5, 6, 7 and 9 σ_{Σ}.

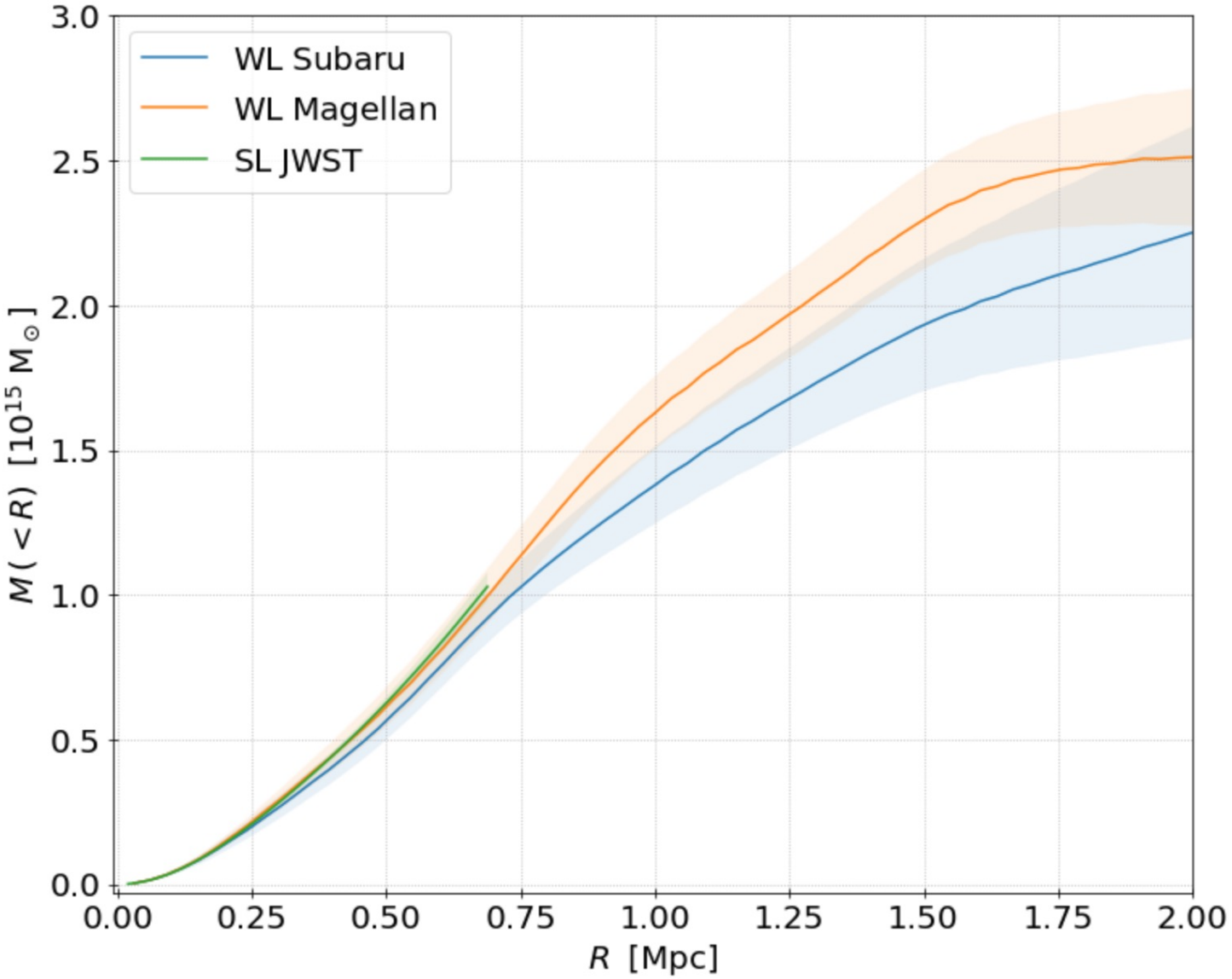

SL : Bergamini et al., 2023

At a distance from the SW BCG of 2 Mpc, the total mass is (2.51 ± 0.24) x 10^{15} $M_\odot$, consistent with the WL study by Medezinski et al., 2016 and our previous analysis based on Subaru/Suprime-Cam data.

We dealt with the ***mass-sheet degeneracy*** by modelling the mass distribution in terms of a cored isothermal ellipsoid

$$\boldsymbol{\Sigma} + c \rightarrow c \approx 0.04 \times 10^{15}\ M_\odot$$

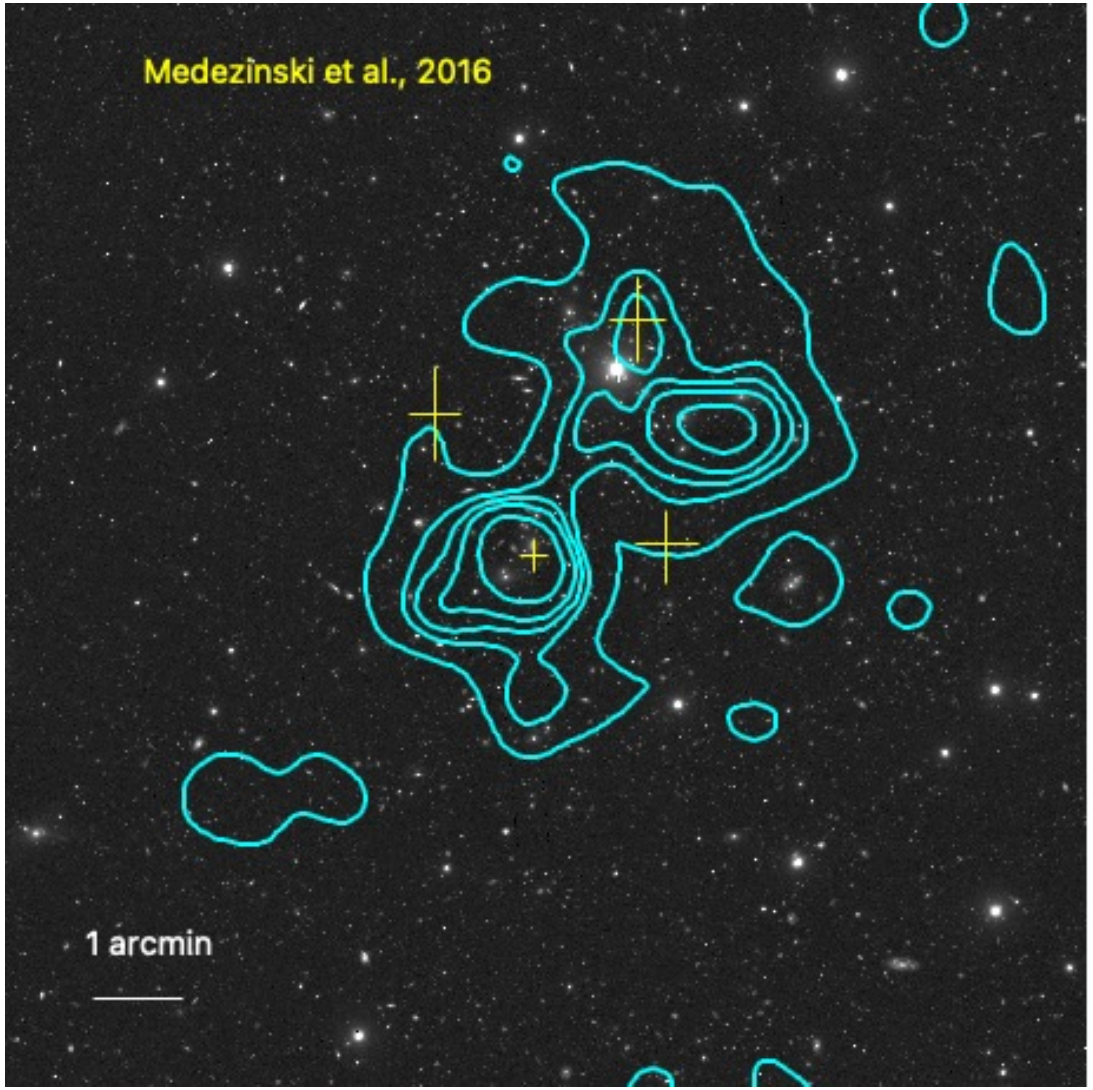

To conclude:

- we reconstructed the total mass distribution of Abell 2744 through WL analysis. The total mass inside 2 Mpc is ≈ 2.51 x 10^{15} $M_{\odot}$.
- we found **three substructures** having a S/N > 7: according to literature, Abell 2744 is not relaxed, but is undergoing a merging process;
- we found a **perfect agreement between** the **SL** (Bergamini et al., 2023) and the **WL** results; i.e., our WL mass distribution is able to extrapolate the SL model at larger radii.

A 6'x6' extract of the composite image with overlaid the **contour lines of the surface mass distribution**. The yellow crosses denote the density peaks detected by Medezinski et al., 2016.

Possible developments:

- further test the robustness of NGMix, e.g., test surface brightness profiles different from the simple exponential model and test the single-band configuration of the software;
- combine several photometric data to estimate photometric redshifts;
- apply different criteria for background and cluster members selection, e.g., using CNNs.

Abell 2744 as seen by NIRCAM @JWST

APPENDIX: SIMULATIONS

We tested on simulated data the robustness of two algorithms: **MCCD** for the PSF recovery and ***NGMix*** for the shape measurement.

We orderly displaced galaxies and stars over a grid and applied no lens.

Each galaxy was modelled in terms of an **exponential surface brightness** profile depending on four parameters.

In each simulation, we varied one of them and kept the others fixed.

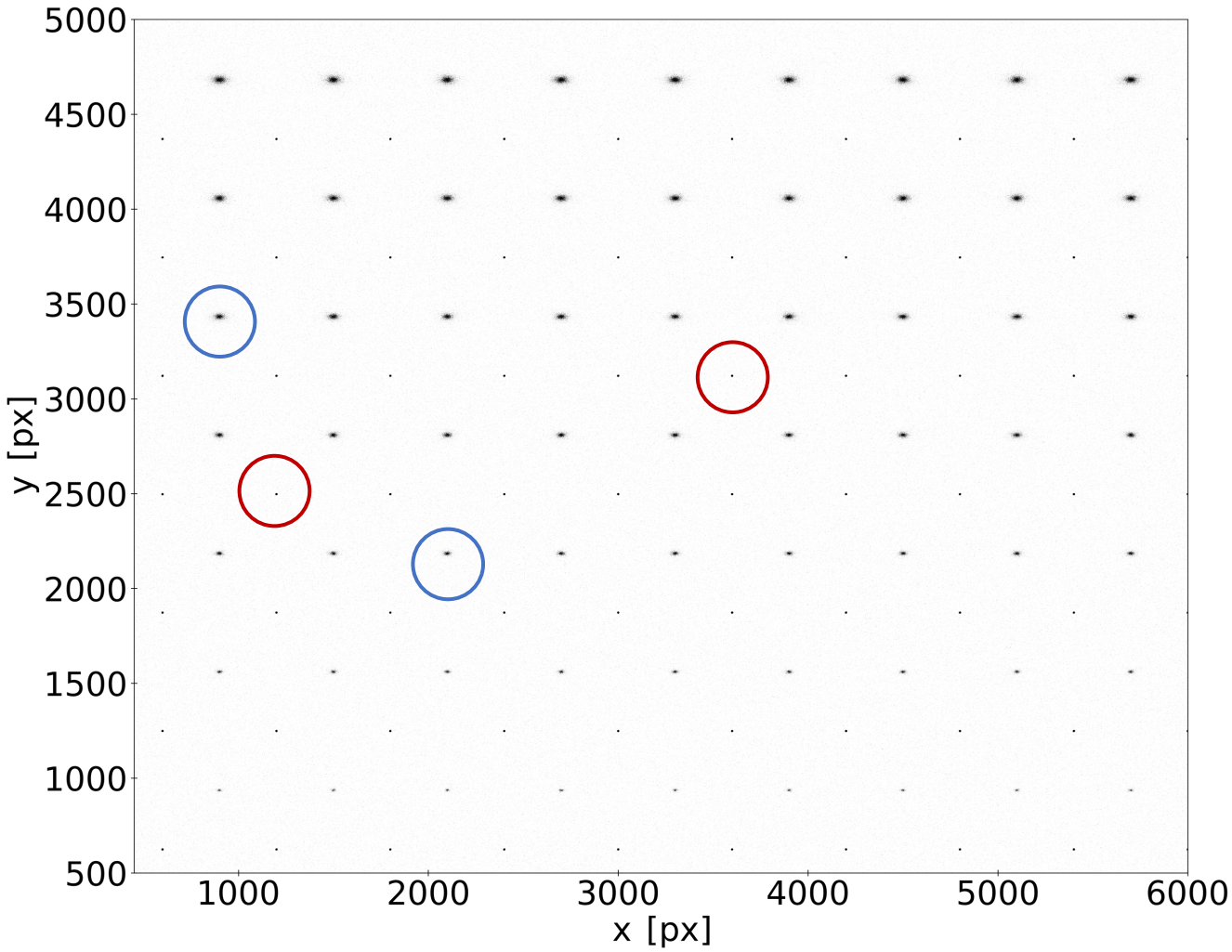

The figure shows an extract of the simulated image with varying exponential length scale.

Through MCCD, the spatial variation of the PSF across the field of view is modelled in terms of a **polynomial**.

The software measures the shapes of the stars and determines the coefficients of the polynomial. Then, it evaluates the PSF at the galaxy positions.

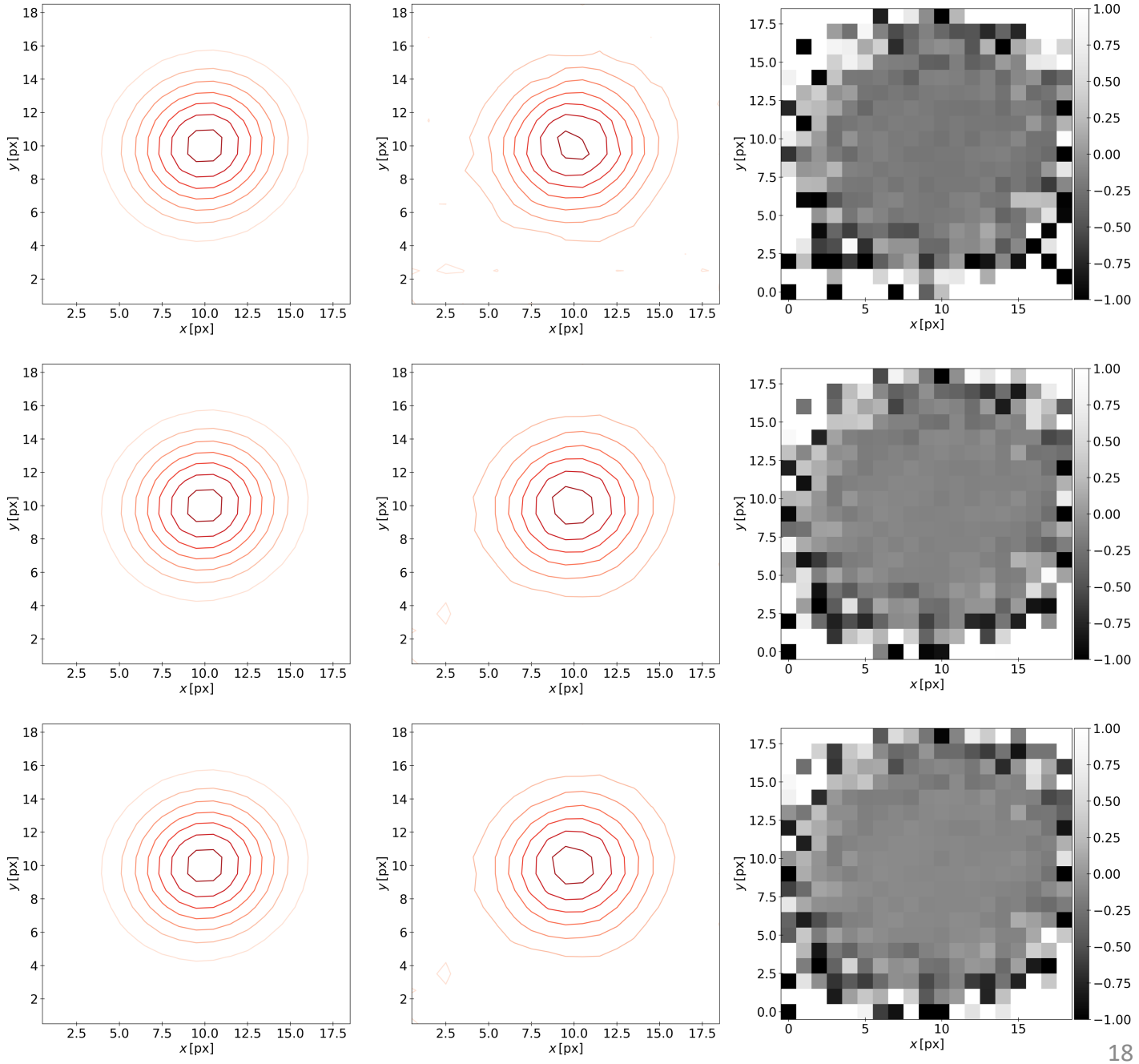

The figure shows the PSF model reconstruction as performed with MCCD.

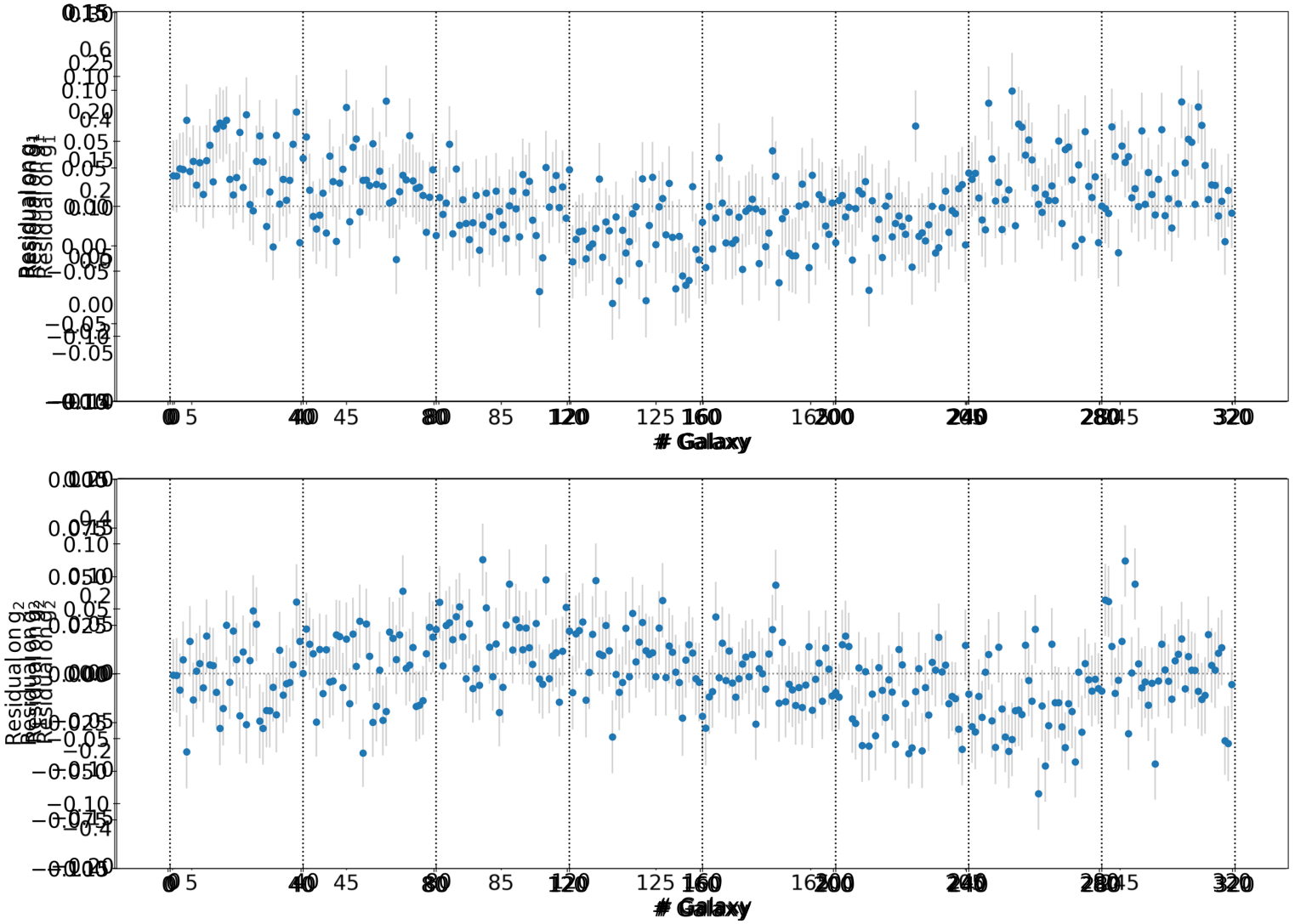

NGMix measures the shapes of the galaxies with a **model fitting approach.**

The fit is best performed if galaxies have:

- **ellipticities** $|\varepsilon| \lesssim 0.7$;
- **central surface brightness** $I \approx 1.5\text{-}2\ I_{sky}$;
- a **size** roughly 1.5 times bigger than the PSF.

No clear dependence on the **inclination angle** was observed.